MEASUREMENT OF CONTACT PRESSURE DISTRIBUTIONS BETWEEN SURFACES BY THERMOELASTICIC STRESS ANALISYS

Roberto MARSILI[1], Nicola BORGARELLI[2]

Università degli Studi di Perugia, Dipartimento di Ingegneria
Via Duranti, 1 - 06125 Perugia, Italy
[1]e-mail: roberto.marsili@unipg.it
[2]e-mail: NBorgarelli@umbragroup.it

Abstract

The development of new techniques for the measurement of contact pressure distributions between bodies in contact is of large interest in mechanics, for the design and verify of many couplings between mechanical components. Examples are the contact between tooth of gears, between the balls and rings of ball bearings, between the wheel and rail etc.

In this paper a new measurement technique is proposed, based on the measurement principle known as thermoelasticity. The particular case about the measurement of contact pressure distribution between a ball and a flat plate is discussed. Previous studies was performed in order to examine the contact surface between the two bodies realizing one of the two bodies in contact using an infrared transparent material, with appropriate values of the other mechanical properties. These studies were anyway only qualitative. In the present work, two calibration methodologies are proposed to obtain measures of contact surface stress between a ball and a flat. One of these methodologies is based on experimental test and the other one is based also on analytic results. The measured stress behaviours are in agreement with the classic Hertz theory; relative uncertainty is smaller than 0.1. This allows to obtain first quantitative results of contact pressure distribution by using thermoelasticity.

Keywords: Contact stress measurement, Thermoelasticity, Hertzian theory, Contact surface

1. INTRODUCTION

The experience shows that the number of the machine's components bring out of order for deterioration of the interacting surfaces is greater than the number of components that failure. Bound problems to the phenomena of fretting, pitting, spalling, share most of the organs in contact (teeth of the gears, ball and roller bearings, cam-tappet system, train's wheels, biomedical outstretched). The study of such phenomena has found an interest always growing for the importance which has in many of engineering and research fields and has today some unknown appearances.

An important aspect for the comprehension of such phenomena is the analysis of the contact pressure. The Hertz's theory supplies a careful distribution of tensions under the ideal contact hypotheses between two solids with simple form. In the current applications the contact is generally more complex, because property of the materials is affected by the shape and the roughness of the surfaces and from the property of the materials. For these reasons is necessary to develop experimental methods for the direct investigation of contact pressure.

Useful help is supplied by the methods of the finite elements (Finite Element Method FEM, Boundary Element Method BEM, etc.) and

moreover from numerical approach combined with inverse analytical one, that allows to evaluate the stress distribution on the surfaces in contact from values measured on a few points of them [8, 9].

A measurement technique which allows to have a global vision of the distribution of the stresses is the photoelasticity. This technique requires the realization of the model of at least one of the elements placed in contact using special materials, so that can be crossed by a polarized light bundle, to highlight the interference fringe groups [5]. Paints sensitive to the pressure and capacitive sensors are able to measure only the stress map distribution with poor resolution [5]. Some successes in the field of the experimental investigation on the bound phenomena to the contact have been done in the last ten years, probably thanks to the development of temperature measurement instruments with high resolution based on no contact methods. Thermographics techniques are able to measure temperature increase on the contact surface generated by the pressure and the creeping speed between two bodies. So it's possible to analyse on their dynamic usury process during sliding friction in dry contact or lubricated conditions [15]. Further studies are still in progress for the determination of thermal maps and the evaluation of the tangential tensions (viscous) in the lubricant film in the contact between sphere and

track in forced lubrication conditions. Realizing one of the two bodies in contact using infrared transparent material, it has been visualized, through infrared thermography, the contact surface [6]. Analogous problems have been faced also with other measure techniques making use of high speed cameras for the determination of the contact surfaces [20]. From the bibliographical research only qualitative tests on temperature field generated by the contact between flat surfaces subject to cyclic tensions have been proposed. [16]. In this work thermoelastic technique is proposed to measure the contact stress between a ball and a flat surface. It is performed an experimental analysis of balls realized in material of engineering interest (strengthened steel, ceramics and plastic materials) employ in technical advanced solutions like the ballscrews for aeronautics applications (flap, slat and stabilizers controller). In order to obtain measures of surface contact stress two calibration methodologies are proposed.

2. DEVELOPMENT OF MEASUREMENT TECHNIQUE

The phenomenon of material changing temperature when it is stretched was first noted by Ghough in 1805 who performed some simple experiments using strand of rubber, but the first observation in metals of what is now known as the thermoelastic effect was made by Weber in 1830: he noted that a sudden change in tension applied to a vibrating wire did not cause the fundamental frequency of the wire to change as suddenly as he expected, but the change took place in a more gradual fashion. He reasoned that this transitory effect was due to a temporary change in temperature of the wire as the higher stress was applied. In 1974, the Admiralty Research Establishment approached Sira Ltd concerning the possibility of determining a relationship between stress and the temperature changes that may be produced by an applied load. Sira confirm feasibility and over the next four years, with funding from English Ministry of Defence, developed a laboratory prototype called Spate (Stress Pattern Analysis by measurement of Thermal Emissions) for application research. The scientific development of the thermoelastic effect, which is well known on gases, where a temperature variation gives a pressure variation, is known in solid materials from little time by the small variation of temperature induced (in the steel where the stress level is near the yield point, the temperature increases of 0.2°C). The thermoelastic technique for the measurement of stress distribution has been developed when a new temperature measurement technique, based on the emission of infrared radiation, with high sensibility, has been discovered. The system consists on a differential thermocamera and on a software for the post processing of the image. The thermocamera

measures the small temperature variation in the mechanical component induced by a dynamic applied load. Thanks to the software it is possible to have the map of stress distribution on the surface of the structure. The resolutions (supplied from the thermoelastic measurement systems) depend on the material characteristics; they are typically 1 MPa for the steel and 0.4 MPa for the aluminium. The structure must dynamically be loaded with frequencies sufficiently high so that the thermodynamic conditions in the material can be considered adiabatic. Under these hypotheses it is possible to have a relationship between the mechanical energy and the thermal energy of the structure. The minimum frequency of the applied load depends on the thermal characteristics of the material and on the gradient of the stress fields. The relationship to determine the sum of the principal stress $\Delta\sigma$ (measured in Pascal) thanks to the thermoelastic principle is:

$$\Delta\sigma = -\frac{D \times R \times \rho \times C_P}{\alpha \times T \times \zeta} \times V \qquad (1)$$

D is the calibration factor measured in °K/Volt, R is a correction factor which compensates for temperature-dependent changes in radiation intensity and wavelength (dimensionless), ρ is the material density measured in kg/m^3, Cp is the specific heat at constant pressure measured in m^2/(s^2 °K), α is the coefficient of thermal expansion measured in 1/°K, T is the temperature measured in °K, ζ is the surface emissivity (dimensionless), and V is the root mean square (RMS) of the signal from the infrared sensor measured in Volt. Commercial thermographic systems are managed by a data acquisition board and a software that returns the value of the thermal field in digital levels (A / D) after acquiring RMS of the signal measured with a 14-bit analog / digital converter. By the thermoelastic technique is possible to measure the map of stress distribution also in complex geometries. Normally it is necessary to paint the surface of the mechanical component to increase and make uniform the emissivity. This no contact technique can have a high spatial resolution, which depends on optical lenses of the thermocamera.

3. TEST BENCH

The stress between a ball and a flat surface it is analysed. Balls of different materials and dimensions, which are employed in the most important engineering applications (steel, ceramic and plastic materials) has been used. In order to increase and to make uniform the emission of the steel ball surface and to avoid reflection phenomena, a superficial chemical treatment was necessary (black oxidation). The common techniques, based on the application of thin black coating to increase the emission coefficient, are inefficient because a contact pressure is present. On the ceramic and plastic materials balls surfaces, the

black coating is not necessary because these materials have an elevated infrared emission coefficient. The test bench to measure the contact stress is schematically shown in figure 1:

A reference ball was put on the load cell which gives the reference signal necessary to synchronize the infrared images acquisitions (figure 1). In order to increase the value of the sinusoidal force applied to the ball, the shaker is connected to a mechanical lever.
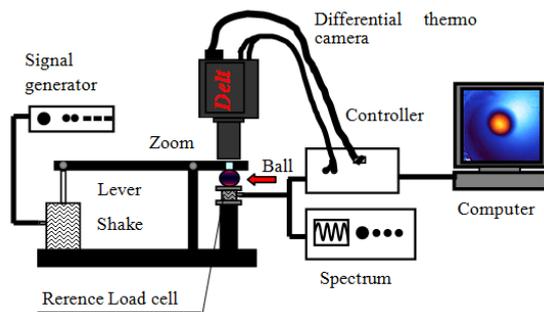

Fig. 1. Test bench to measure the contact stress.

A signal generator is used to drive the shaker and the load cell signal is acquired by a spectrum analyser. In order to have the optical access, in the contact point of the mechanical lever there is a hole where a flat transparent infrared material (Polystyrene) is fixed. The infrared emission of the ball contact area crosses the polystyrene flat it is acquired by the differential thermocamera. No tests have been done to estimate the thermocamera uncertainty; the system constructor give a resolution of 1 mK after 30 seconds of acquisition and a NDTE less than 18mK [Delta Vision Handbook]. The wavelength spectral range of the thermocamera is 3 ¸ 5 μm. Because of the contact area between the plan and the balls is very little (smaller than a millimetre) an optical zoom is used which has 320 x 256 measurement points on an area of 3.8 X 3.1 millimetres; this allows to obtain a spatial resolution of 12 μm. In order to have some stress distribution to compare, the tests are carried out with different load amplitude and different frequencies. The external load is sinusoidal with amplitudes between 5 and 20 N, depending on the balls dimensions.

3. RESULTS ANALYSIS

In the figure 2 and 3 a typical stress distribution measured on the contact area is shown in terms of emitted infrared radiation:
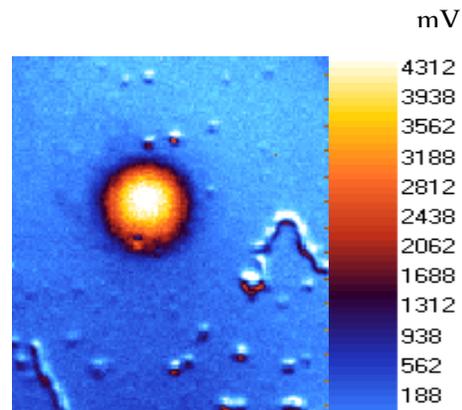

Fig. 2. Typical example of the distribution of the intensity radiation emitted from the ceramic ball surface (ball diameter 6.35 mm, applied load 10N).
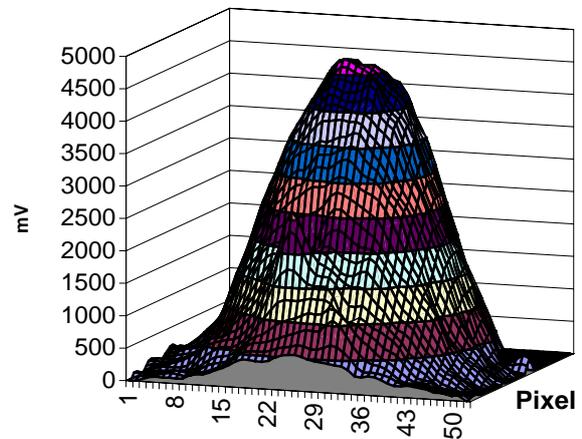

Fig. 3. Typical example of the 3D distribution of the intensity radiation emitted from the ceramic ball surface (ball diameter 6.35 mm, applied load 10N).

It is possible to see axial-symmetric behaviours with the maximum value at the centre of the contact area. The values decrease and become zero at the contact area boundary. In the figures 4 and 5 the stress behaviours along the diameter of the contact area is compared.

From the comparison between the stress behaviours on the contact area of different material balls, which is loaded by the same load, it is possible to see a very different absolute emission value. These values come not from a so high different in stress level, but from a different emission coefficient and thermoelastic material characteristics. Moreover it is possible to see the different dimensions of the contact areas when the ball size and the amplitude of the applied load change.
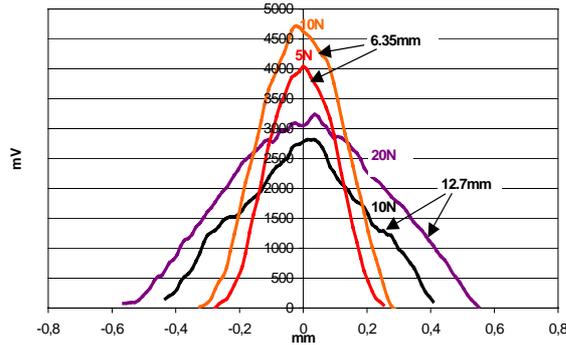
Fig. 4. Typical intensity radiation behaviours along the diameter of the contact area on the ceramic balls (balls diameter 6.35 mm and 12.70 mm).
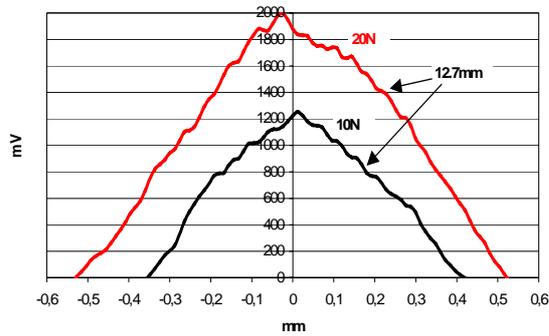

Fig. 5. Typical intensity radiation behaviours along the diameter of the contact area on the steel ball (ball diameter 12.70 mm).

Thanks to the Hertzian theory is possible to calculate the maximum stress and radius a of the contact area as shown [20]:

$$p_{max} = \frac{3}{2}\left(\frac{P}{\pi a^2}\right) \quad (2)$$

$$a = 0.721\sqrt[3]{PDC_E} \quad (3)$$

$$\text{with } C_E = \frac{1-v_1^2}{E_1} + \frac{1-v_2^2}{E_2} \quad (4)$$

where P is the applied load, D is the ball diameter and C_E is function of the Poisson and Young modulus of the two materials in contact. The stress behaviours on the contact surface is expressed in cylindrical coordinates as shown (5) (6) (7):

$$\sigma_{\vartheta}(r) = p_{max}\left[-\frac{1-2v}{3}\frac{a^2}{r^2}\left[1-\left(1-\frac{r^2}{a^2}\right)^{3/2}\right]-2v\left(1-\frac{r^2}{a^2}\right)^{1/2}\right] \quad (5)$$

$$\sigma_r(r) = p_{max}\left[\frac{1-2v}{3}\frac{a^2}{r^2}\left[1-\left(1-\frac{r^2}{a^2}\right)^{3/2}\right]-\left(1-\frac{r^2}{a^2}\right)^{1/2}\right] \quad (6)$$

$$\sigma_z(r) = -p_{max}\left(1-\frac{r^2}{a^2}\right)^{1/2} \quad (7)$$

Thanks to the relationship (1) in each point is:

$$\Delta\sigma = \sigma_r + \sigma_{\vartheta} + \sigma_z = K \times V \quad (8)$$

where K is the calibration factor of the thermoelastic system, V is the RMS of the signal measured by the infrared sensor and $\Delta\sigma$ is the sum of the principal stresses calculated by the relationships (5) (6) and (7), known the value of P measured by the load cell. Integrating the relationships (8) on the contact area it is obtained:

$$K = \frac{\int_A (\sigma_r + \sigma_{\vartheta} + \sigma_z)dA}{\int_A VdA} \quad (9)$$

Repeated measurements varying the applied load between 5 and 20 N, allow to determine the best available estimate of the expected value of the thermoelastic constant $\bar{k}$ and the experimental standard deviation of the mean $s(\bar{k})$. In this case is:

$\bar{k}$ = 0.10 MPa/mV and $s(\bar{k})$ = 0.01 MPa/mV, for the ceramic material.

$\bar{k}$ = 0.13 MPa/mV, $s(\bar{k})$ = 0.01 MPa/mV, for the steel.

In such a way it's possible to express the results obtained for the balls in different material directly in terms of stress, multiplying the values of the infrared intensity radiation measured by the determined thermoelastic constant $\bar{k}$.

4. EXPERIMENTAL CALIBRATION AND UNCERTAINTY ANALYSIS

Normally in the thermoelastic measures the calibration comes measuring the deformation by a strain gauge rosette in a point of the structure. So the calibration factor is:

$$K = \frac{E(\varepsilon_x + \varepsilon_y)}{V(1-v)} \quad (10)$$

where E is the Young modulus of the material, v is the Poisson modulus, $(\varepsilon_x + \varepsilon_y)$ is the sum of the principal strains and V is the RMS of the signal measured by the infrared sensor. Because it is impossible to apply the strain gauges in the contact area between a ball and a plan, the calibration is done using specimens of the same material and with the same emissivity characteristics of the balls. These specimens are beams which are fixed at one end and loaded at other one applying a sinusoidal load to have the same stress level measured on the balls. Repeated measurements of the principal strains on the same area of the beam and the relative measure of the infrared intensity radiation, allow to estimate the calibration factor K (10). Repeated measurements varying the applied load, the observation area and the excitation frequency (between 0 and 15,50 Hz) it is possible to have the best available estimate of the thermoelastic constant $\bar{k}$ expected value:

$\bar{k}$ = 0,11 MPa/mV   for the ceramic material

$\bar{k}$ = 0,14 MPa/mV   for the steel

The experimental standard deviation is $s(\bar{k}) = 0.01$ MPa/mV.

It is possible to see how the values of the thermolastic constant are compatible with the values estimated in the previous paragraph.

From the comparison between the stress measured distribution and the Hertzian theory stress distribution is possible to see, in figure 6 and 7, a good agreement of the stress behaviours and of the contact area dimension when the applied load changes. At the centre of the contact area, where the stress level is high, the two behaviours are nearly coincident. The stress level on the contact area boundary is greater than the Hertzian stress and with a lower gradient. This behaviour gives a greater contact area than the Hertzian one. It is probably caused to the small entity of the stress level which is near to the resolution of the instrument. However the stress behaviours near the area boundary calculated by the Hertzian theory has a too high gradient, which is not realistic from the physical point of view.
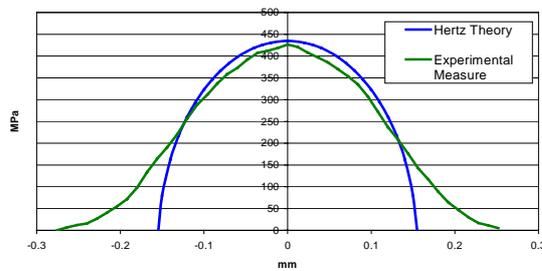

Fig. 6. Comparison between the measured stress distribution and Hertzian theory along the contact area diameter on the ceramic ball (ball diameter 6.35 mm, applied load 5 N).
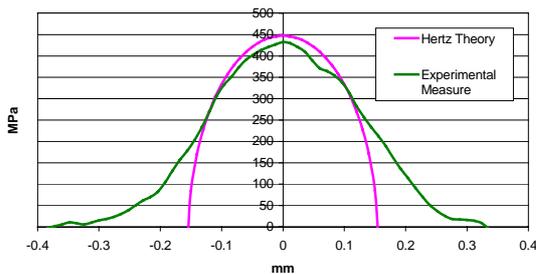

Fig. 7. Comparison between the measured stress distribution and Hertzian theory along the contact area diameter on the steel ball (ball diameter 6.35 mm, applied load 5 N).

The composed uncertainty type A on the value of the thermolastic constant K can be determined basing on relationship (10) as follow (11):

$$\partial K = \left| \frac{\partial K(E)}{\partial E} \partial E \right| + \left| \frac{\partial K(\varepsilon_x)}{\partial \varepsilon_x} \partial \varepsilon_x \right| + \left| \frac{\partial K(\varepsilon_y)}{\partial \varepsilon_y} \partial \varepsilon_y \right| + \left| \frac{\partial K(V)}{\partial V} \partial V \right| + \left| \frac{\partial K(\nu)}{\partial \nu} \partial \nu \right|$$
(11)

Assuming an relative uncertainty of 2% on the Poisson and Young modulus of the materials, of 2%

on the determination of the principal strain ε and 2% on the RMS of the signal measured by the infrared sensor *V*, the combined standard uncertainty is $\partial K = 0.009$, and so relative uncertainty is

$$\frac{\partial K}{K} = 9\%$$
(12)

6. CONCLUSIONS

The stress distribution on a mechanical component which is loaded by a sinusoidal load can be studied by thermoelastic analysis. It is possible to emphasize how is easy to measure the qualitative stress distribution also on complex surfaces. The goal of this work is the development of a new technique, based on the application of the thermoelastic principle, to measure the contact stress distribution between a ball and a plan. The experimental tests on reference balls of different material and size have evidenced a good agreement between the measure results and the Hertzian theory. The difficulty to have the experimental reference values to characterize the thermoelastic system, has carried out the development of two different approaches for the determination of the calibration factor of the system. Following the two methodologies is possible to establish a thermoelastic constant k = 0.13 MPa/mV for the steel and k = 0.11 MPa/mV for the ceramic material with an expanded uncertainty of 0.02 MPa/mV, assuming 2 the coverage factor. It also necessary to underline the stress distribution measured by the thermoelastic analysis is relative to the surface of the mechanical components and it is expressed in terms of sum of principal stress. However it is possible to know the single stress components using the thermoelastic analysis together with known numerical techniques (FEM, BEM).

REFERENCES

1. Barone S, Patterson EA. An iterative, finite difference method for post-processing thermoelastic data using compatibility", Journal of Strain Analysis for Engineering Design, 1998; 33(6): 437-447.
2. Becchetti M, Flori R, Marsili R, Rossi G. Stress and strain measurements by image correlation and Thermoelasticity. Society for Experimental Mechanics - SEM Annual Conference and Exposition on Experimental and Applied Mechanics 2009, 2009; 1: 70-75
3. Garinei A, Marsili R. Development of a new capacitive matrix for pressure distribution measurement. International Journal of Industrial Ergonomics, 2014; 44(1):114-119 doi: 10.1016/j.ergon.2013.11.012.
4. Grigg JS, Dulieu-Barton JM, Shenoi RA. Validation of a complex composite construction using thermoelastic stress analysis, Proceedings of the SEM IX International Congress on Experimental Mechanics, 2000; 5-8: 355-358.
5. Harwood N, Cummings WM. Thermoelastic Stress Analysis. Adam Hilger 1991.
6. Harish G, Szolwinski MP, Farris TN, Sakagami T.

Evaluation of fretting stress through full-field temperature measurement. ASTM STP 2000.

7. Brustenga G, Marsili R, Moretti M, Pirisinu J, Rossi, G. Measurement on rotating mechanical component by thermoelasticity. Journal Applied Mechanics and Materials, 2005; 3-4: 337-342.

8. Marsili R, Moretti M, Rossi G. Thermoelastic Modal Stress Analysis", IMAC XXVI Conference & Exposition on Structural Dynamic, Orlando, Florida, 2008.

9. Ju SH, Lesniak JR, Sandor BI, Numerical simulation of stress intensity factors via the thermoelastic technique, Experimental Mechanics, 1997; 37(3):278-284.

10. Lesniak JR, Thermoelastic data improvements, Proceedings of 1993 SEM Spring Conference on Experimental Mechanics, Dearborn, Michigan, 1993: 721-729.

11. Garinei A, Marsili R. Design of an optical measurement system for dynamic testing of electrospindles", Measurement, 2013; 46(5): 1715-1721. DOI: 10.1016/j.measurement.2013.01.006.

12. Offermann, S, Beaudoin JL, Bissieux C, Frick H, Thermoelastic Stress Analysis Under Non-adiabatic Conditions, Experimental Mechanics, 1997; 37(4): 409-413.

13. Cardelli E, Faba A, Marsili R, Rossi G, Tomassini R. Magnetic nondestructive testing of rotor blade tips, Journal of Applied Physics, 2015; 117, 17A705 doi: 10.1063/1.4907180.

14. Becchetti M, Flori R, Marsili R, Moretti M. Comparison between digital image correlation and thermoelasticity for strain field analysis. 9th International Conference on Vibration Measurements by Laser and Noncontact Techniques and Short Course; Ancona; Italy; Conference Proceedings, 2010; 1253: 233-240.

15. Marsili R, Brustenga G, Moretti M, Pirisinu J, Rossi G.Measurement on rotating mechanical component by thermoelasticity", Journal Applied Mechanics and Materials,2005; 3-4: 337-342.

16. Reifsnider KL, Williams RS. Determination of fatigue-related heat emission in composite materials. Experimental Mechanics, 1974: 479-485.

17. Rocca R, Bever MB. The Thermoelastic Effect in Iron and Nickel (As a Function of Temperature), Trans. AIME, 1950; 188: 327-333.

18. Sakagami T, Ogura K, Shoda M. Thermal sensing and imaging of the dry sliding contact surface, Orlando Florida SPIE 1995.

19. Garinei A, Marsili R. Thermoelastic Stress Analysis of the Contact Between a Flat Plate and a Cylinder, Measurement: Journal of the International Measurement Confederation, 2014; 52 (1):102-110. http://dx.doi.org/10.1016/j.measurement.2014.03.005

20. Brouckaert JF, Marsili R, Rossi G. Development and experimental characterization of a new non contact sensor, 10th International Conference on Vibration Measurements by Laser and Noncontact Techniques - AIVELA, Ancona, Conference Proceedings, 2012; 1457: 61-68. DOI: 10.1063/1.4730543.

21. Garinei A, Marsili R. A new diagnostic technique for ball screw actuators, Measrement, 2012; 45(5): 819-828, DOI: 10.1016/j.measurement.2012.02.23.

22. Szolwinski MP, Harish G, Farris TN. In-Situ measurement of near surface fretting contact temperatures in an aluminium alloy. Journal of Tribology, 1999;121.

23. Brouckaert J, Marsili R, Rossi G. Development and experimental characterization of a new non contact sensor for blade tip timing, 10th International Conference on Vibration Measurements by Laser and Noncontact Techniques - AIVELA, Ancona, Conference Proceedings, 2012; 1457: 61 - 68 DOI: 10.1063/1.4730543.

24. Tritschler B, Forest B, Rieu J. Application de la theorie de Hertz au cas d'un contact polymere/metal", Ecole Nationale Superieure des Mines de Saint- Etienne Centre.

25. UNI CEI ENV 13005. Guide to the expression of uncertainty in measurement. July 2000.

26. Wong AK, Dunn SA, Sparrow JG, Residual stress measurement by means of the thermoelastic effect, Nature, 1988; 332: 613-615.

27. D'Emilia G, Lucci S, Natale E, Pizzicannella F. Validation of a Method for Composition Measurement of a Non-Standard Liquid Fuel for Emission Factor Evaluation, MEASUREMENT, 2011; 44: 18-23.

28. D'Emilia G, Razzè L, Zappa E. Uncertainty Evaluation of High Frequency Image-Based Vibration Measurement, Measurement, 2013; 46(8): 2630-2637.

29. D'Emilia G, Di Rosso G, Gaspari A, Massimo A. Metrological interpretation of a six sigma action for improving on line optical measurement of turbocharger dimensions in the automotive industry. Proceedings of the Institution of Mechanical Engineering: Part D, Journal of Automobile Engineering, 2015; 229(2): 261-269, DOI: 10.1177/0954407014539671.

30. D'Aponte F, D'Emilia G, Lupinetti S, Natale E, Pasqualoni P. Uncertainty of slip measurements in a cutting system of converting machinery for diapers production, Int. J. Metrol. Qual. Eng., 2015; 6(3): 1-6.

31. Speranzini E, Agnetti S, Corradi M. Experimental analysis of adhesion phenomena in fibre-reinforced glass structures", Composites part B 2016, 101:155-166. 2016. DOI: 10.1016/j.compositesb.2016.06.074.

32. Speranzini, E. Tralascia S. Engineered Lumber: LVL and Solid Wood Reinforced with Natural Fibres. In Proceedings of the WCTE 2010—Word Conference on Timber Engineering, Trento, Italy, 2010: 1685–1690.

33. Speranzini E, Agnetti S. Structural performance of natural fibers reinforced timber beams. In Proceedings of the 6th International Conference on FRP Composites in Civil Engineering—CICE2012, Roma, Italy, 2012.

34. Corradi M, Borri A, Castori G, Speranzini E. Fully reversible reinforcement of softwood beams with unbounded composite plates. Composite Structures 2016, 149:54-68. DOI: 10.1016/j.compstruct.2016.04.014

Roberto MARSILI is Researcher of Mechanical Measurements at University of Perugia. He is graduated in Mechanical Engineering and he obtained the PhD degree from University of Padova studying piezoelectric films. His area of interest regards diagnostics of mechanical systems, thermoelastic stress analysis.

Nicola BORGARELLI is Technical Manager of Umbra Group of Perugia. He is graduated in Mechanical Engineering and he obtained the PhD degree. His area of interest regards ball recirculation screws and bearings.